Geophysical Research Letters

RESEARCH LETTER
10.1029/2022GL100257

Key Points:

- Increasing aridity on the southeast coast of China from 4.7 to 3.8 ka captured by the hydrogen isotope compositions (δD) of leaf waxes
- The abrupt drying is mainly shaped by a more El Niño-like state over the tropical Pacific Ocean during the mid-to-late Holocene transition
- Such a shift in hydroclimate might have promoted the development of mixed rice and millet farming on the southeast coast of China

Supporting Information:

Supporting Information may be found in the online version of this article.

Correspondence to:

X. Huang,
xyhuang@cug.edu.cn

Citation:

Wang, X., Huang, X., Zhao, H., & Sachse, D. (2022). Abrupt drying on the southeast coast of China during the mid-to-late Holocene transition. *Geophysical Research Letters*, *49*, e2022GL100257. https://doi.org/10.1029/2022GL100257

Received 30 JUN 2022
Accepted 20 NOV 2022

Abrupt Drying on the Southeast Coast of China During the Mid-to-Late Holocene Transition

Xinxin Wang[1,2], Xianyu Huang[3], Hongyan Zhao[4], and Dirk Sachse[2]

[1]Institute of Palaeontology, Yunnan Key Laboratory for Palaeobiology, Yunnan Key Laboratory of Earth System Science, Yunnan University, Kunming, China, [2]Geomorphology Section, GFZ-German Research Centre for Geosciences, Potsdam, Germany, [3]State Key Laboratory of Biogeology and Environmental Geology, China University of Geosciences, Wuhan, China, [4]State Environmental Protection Key Laboratory of Wetland Ecology and Vegetation Restoration, Northeast Normal University, Changchun, China

Abstract It is becoming increasingly clear that China experienced significant hydrological changes during the mid-to-late Holocene transition—a period characterized by societal changes. However, the nature of the hydroclimate anomaly as well as the direct consequences on societies in Southeast China remains unclear. Here, we present a leaf wax record from the Shuizhuyang peat deposit in Southeast China spanning the Holocene. The δD values of C_{29} *n*-alkane (δD_{C29}) showed a large positive shift up to 24‰ from 4.7 to 3.8 ka, which changed independent of vegetation proxies and could not be solely explained by precipitation δD variations. It is thus most likely to reflect abrupt drying, which is probably shaped by a more El Niño-like mean state in the tropical Pacific Ocean. We hypothesize that such a significant change in hydroclimate might have promoted the development of mixed rice and millet farming on the southeast coast of China.

Plain Language Summary The mid-to-late Holocene transition with significant changes in climate and agriculture-based civilization affords a valuable insight into abrupt climate changes and human adaption. Increasing studies have shown large shifts in hydrological regime in China during this critical transition. However, the hydrological expression and its potential impact on the agriculture practice in Southeast China remains unclear. In this study, we utilize the hydrogen isotope compositions (δD) of leaf waxes from the Shuizhuyang peat deposit on the southeast coast of China to reconstruct hydrological changes during the mid-to-late Holocene transition. We find that the mid-to-late Holocene transition on the southeast coast of China is characterized by an abrupt drying, which is primarily modulated by a more El Niño-like mean state over the tropical Pacific Ocean. Such a significant change in hydroclimate might have promoted the development of mixed rice and millet farming on the southeast coast of China coeval to the mid-to-late Holocene hydrological shift.

1. Introduction

The mid-to-late Holocene transition with the 4.2 ka event as the chronological divider (Walker et al., 2018) witnessed severe climate deteriorations all over the world, but in particular the tropical and subtropical areas (Bini et al., 2019; Cullen et al., 2000; Dixit et al., 2014; Renssen, 2022). Those climatic changes have been linked to the demise of ancient civilizations in ancient Egypt, Mesopotamia and the Indus Valley (Weiss, 2016). In China, this transition also coincides with the transformation of major agriculture-based Neolithic cultures (F. Liu & Feng, 2012; Sun et al., 2019). However, the climate anomaly associated with shifts in the hydrological regime during this critical transition in the East Asian summer monsoon (EASM) regions of China has not been fully understood, in part due to apparently conflicting results over space and lacking records from key regions. Hydrological records from North China generally show a distinct drought (F. Chen et al., 2015), while mounting evidence from the middle and lower reaches of the Yangtze River suggests a wet interval (Zhang, Cheng, et al., 2018; Innes et al., 2014; Xie et al., 2013). On the southeast coast of China, the hydrological expression remains unclear due to a paucity of independent hydrological records (X. Wang & Huang, 2019). This region is in the frontal zone of the EASM and thus is particularly sensitive to the hydroclimate changes related to the EASM (Zhang, Jiang, et al., 2021). Besides, it is a key point in the dispersal route of agriculture to Southeast Asia during the mid-late Holocene (Ma et al., 2020). To fill this gap, it is essential to explore hydrological changes on the southeast coast of China during the mid-to-late Holocene transition and further assess its driving mechanisms and the potential impact this change had on agriculture development.

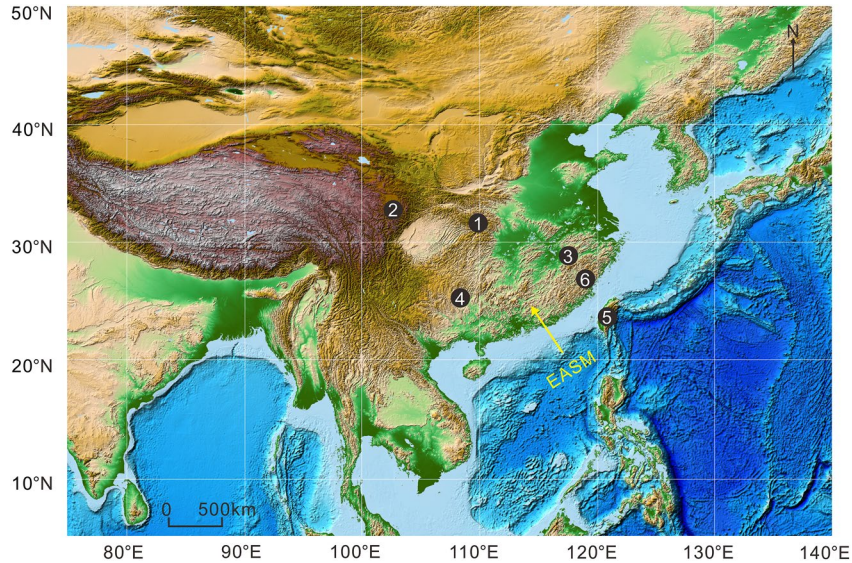

Figure 1. Locations of the Shuizhuyang peat deposit and other key sites mentioned in the text. 1: Dajiuhu peatland (Xie et al., 2013); 2: Hongyuan peatland (Seki et al., 2011); 3: Shennong Cave (Zhang, Cheng, et al., 2018); 4: Dongge Cave (Dykoski et al., 2005); 5: Toushe Basin (Z. Huang et al., 2020), and 6: Shuizhuyang peat deposit (this study).

The Shuizhuyang peat deposit is located in Fujian Province on the southeast coast of China. According to previous studies, its successive sedimentation covers the entire Holocene, which enables continuous record of climate changes (X. Wang & Huang, 2019; Yue et al., 2012). Prior studies based on pollen and bacterial branched glycerol dialkyl glycerol tetraethers from the Shuizhuyang peat deposit have revealed Holocene vegetation and temperature history, which point to a major climate reorganization during the mid-to-late Holocene transition (M. Wang et al., 2017; Yue et al., 2012). Our previous work has reconstructed hydrological changes over the Holocene based mainly on microbial hopanoids from the Shuizhuyang peat deposit, but with a relatively coarse resolution during the mid-to-late Holocene (X. Wang & Huang, 2019).

Terrestrial plant leaf wax *n*-alkane δD values have been emerging as particularly useful tracers for precipitation as they are tightly correlated with the δD values of precipitation (δD_p) (e.g., Feakins et al., 2016; McFarlin et al., 2019; Sachse et al., 2012). In this study, we derive a new leaf wax biomarker record over the Holocene from the Shuizhuyang peat deposit. The δD values of leaf wax are utilized to reconstruct hydrological changes. Further, climatological drivers and the repercussions of the hydroclimate changes on the agricultural practice of the region are explored.

2. Materials and Methods

2.1. Materials

The Shuizhuyang peat deposit lies near the border of Pingnan and Gutian County in the northeastern Fujian province. This area is characterized by a subtropical monsoon climate. The EASM generally begins in mid-May and withdraws in September (Ding & Chan, 2005). At the adjacent Pingnan meteorological station, the annual mean temperature and precipitation is 15°C and ∼1,800 mm, respectively. In May 2018, a 2.73-m-long peat core (abbr. SZY18; 26°46′27″N and 119°2′41″E; 990 m above sea level; Figure 1 and Figure S1 in Supporting Information S1) was collected from the Shuizhuyang peat deposit and sliced at 1 cm interval in the field. The lithology of the SZY18 core is as below: 0–30 cm: cultivated soil; 30–195 cm: brown-black peat with visible plant debris; 195–200 cm: gray black peat; 200–220 cm: light brown black peat; and 220–273 cm: brown-black to gray-black peat (Figure S1 in Supporting Information S1).

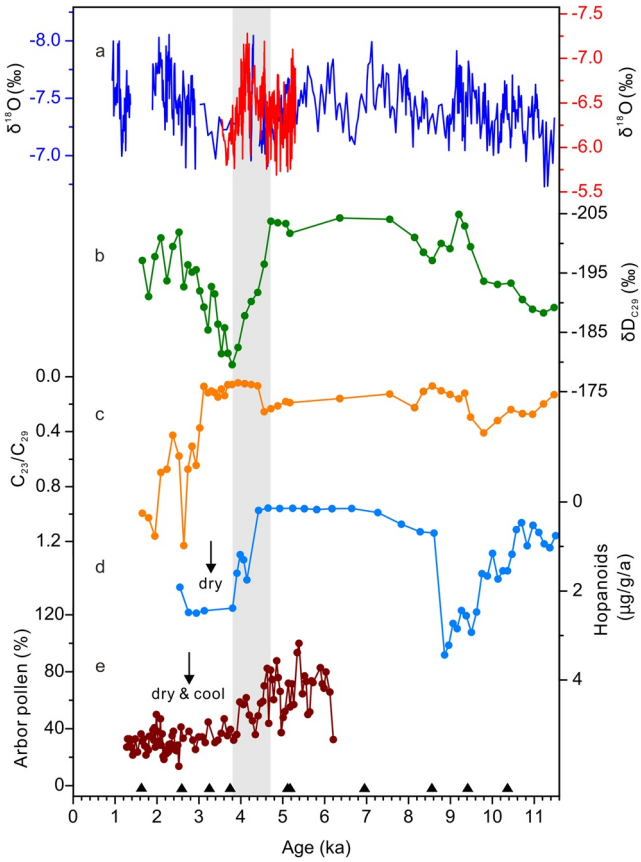

Figure 2. Comparisons of SZY18 records and paleoclimate records from monsoonal China. (a) Stalagmite $\delta^{18}O$ records from Shennong Cave over the Holocene (left *y*-axis, Zhang, Zhang, et al., 2021) and during 5.3 and 3.5 ka (right *y*-axis, Zhang, Cheng, et al., 2021); (b) SZY18 δD_{C29}; (c) SZY18 C_{23}/C_{29}; (d) hopanoid flux from the Shuizhuyang peat deposit (X. Wang & Huang, 2019); and (e) arbor pollen percentage from the Toushe Basin in central Taiwan (Z. Huang et al., 2020). Age control points of the SZY18 core are shown along the *x*-axis. The gray shade indicates the transitional period.

2.2. Methods

The chronology of the SZY18 core is well constrained by 12 radiocarbon dating points (Table S1 in Supporting Information S1). Recognizable plant residues from 12 peat layers in the SZY18 core were sent to Beta Analytic Radiocarbon Dating Laboratory for AMS ^{14}C dating. ^{14}C dates were converted to calendar years before the present using the INTCAL20 calibration database (Reimer et al., 2020). The age model was built using a Bayesian approach (Blaauw & Christen, 2011).

Lipid extraction and separation were achieved by using ultrasonic extraction and silica gel column chromatography, with procedures identical to Wang and Huang (2019), in the State Key Laboratory of Biogeology and Environmental Geology, China University of Geosciences at Wuhan. *n*-Alkane measurements were conducted in the Organic Surface Geochemistry Laboratory of GFZ-German Research Centre for Geosciences, followed Rach et al. (2020). *n*-Alkane identification and quantification were performed on an Agilent 7890 gas chromatograph (GC) coupled to a flame ionization detector and Agilent 5975 mass selective detector. Compound-specific hydrogen isotope measurements of *n*-alkanes were performed on a Trace GC 1310 connected to Delta V plus isotope ratio mass spectrometer (Thermo Fisher Scientific). The δD results were transferred to the VSMOW scale (Text S2 in Supporting Information S1). Reproducibility for specific compounds was better than 5‰, based on at least duplicate analyses.

A new time series of stalagmite $\delta^{18}O$ from Shennong Cave (28°42′N and 117°150′E; 383 m a.s.l.; Figure 1; Zhang, Zhang, et al., 2021) was obtained by the cubic spline interpolation with Matlab R2016a software (The MathWorks Inc., USA), to facilitate correlation analysis with the same time vector as SZY18 δD record. Correlation analysis was performed with SPSS 20.0 software (International Business Machines Co., USA).

3. Results

The age-depth model shows the SZY18 core was dated back to ~12.9 ka and the upper 237–40 cm peat layer for biomarker analysis covered the interval of 11.5–1.6 ka (Table S1 and Figure S1 in Supporting Information S1). The chronology of SZY18 core is broadly consistent with the age frame of previous peat cores retrieved from the same peat deposit (X. Wang & Huang, 2019; Yue et al., 2012). The average sedimentation rate fluctuated between 0.12 and 0.16 mm/a from 11.5 to 9.4 ka, and remained at very low values between 0.02 and 0.07 mm/a from 9.4 to 5.2 ka. After that, the average sedimentation rate increased significantly and varied between 0.20 and 0.76 mm/a.

n-Alkanes in peat samples distributed from C_{21} to C_{35} and peaked at C_{25} and C_{29} (Figure S2 in Supporting Information S1). The ratio of C_{23} to C_{29} *n*-alkanes (C_{23}/C_{29}) fluctuated between 0.04 and 0.41 from 11.5 to 3.1 ka before rising to 1.23 at 2.6 ka. C_{23}/C_{29} varied significantly between 0.43 and 1.16 afterward (Figure 2). The δD values of C_{25} and C_{29} *n*-alkanes (δD_{C25} and δD_{C29}) ranged from −211‰ to −180‰ and shared a similar pattern ($r = 0.64$, $p < 0.01$) (Table S3 and Text S3 in Supporting Information S1). On the whole, the δD values gradually declined during the early Holocene and stayed at more negative values during the mid-Holocene. Then they increased rapidly from 4.7 ka to 3.8 ka with the excursion amplitudes between 24‰ and 26‰, followed by a drop until 2.5 ka. The δD values tended to level off afterward (Figure S3 in Supporting Information S1).

4. Discussion

4.1. Hydrological Reconstruction

In the SZY18 core, *n*-alkane distributions are characterized by a dominance of C_{25} and C_{29} over the range of C_{21} to C_{35}. A dominance of C_{25} and C_{29} *n*-alkanes has been reported previously in peats (e.g., Andersson et al., 2011; X. Huang et al., 2016). Typically, C_{29} *n*-alkane is derived from vascular plants, while C_{23} and C_{25} *n*-alkanes possibly originate from *Sphagnum* or other plants in peatland settings (Nichols et al., 2006; Zhao et al., 2018). As C_{29} *n*-alkane has a clear source (Zhao et al., 2018), it is selected as the focus of this study for the following discussion.

In peatlands, peat-forming vascular plants mainly utilize soil water as H source for photosynthesis (Huang & Meyers, 2019). The δD values of their leaf wax *n*-alkanes are primarily controlled by δD_p, plant life-form types and evapotranspiration (Huang & Meyers, 2019; J. Liu & An, 2018; Sachse et al., 2012).

In Southeast China, δD_p could be influenced by the D-depleted typhoon rains (Xu et al., 2019). However, it is unlikely that typhoon rains have exerted an important influence on SZY18 δD_{C29} during the mid-to-late Holocene transition. First, no layers of silty peat indicative of floods resulting from tropical cyclones have been observed in the SZY18 peat core (Figure S1 in Supporting Information S1). Second, a paleo-typhoon record from northeastern Taiwan showed a quite low frequency of typhoon activities during the mid-to-late Holocene transition (H. F. Chen et al., 2012). Third, the impact of tropical cyclone events generally lasts only for a couple of days (Xu et al., 2019), contrasting with the sample resolution (ca. 50 years) in the SZY18 core. Thus, the footprint of tropical cyclone events is not necessarily captured by the SZY18 δD_{C29} signal.

To further assess the influence of δD_p variations, the SZY18 δD_{C29} record is compared to the stalagmite $\delta^{18}O$ results from Shennong Cave (~280 km northwest to the Shuizhuyang peat deposit; Zhang, Cheng, et al., 2021; Zhang, Zhang, et al., 2021; Figure 1). In the monsoon regions of China, stalagmite $\delta^{18}O$ records are primarily a signal of precipitation $\delta^{18}O$, which is largely controlled by the large-scale atmospheric circulation (X. Liu et al., 2020; Tan, 2014). This is well supported by the similar overall trends among stalagmite $\delta^{18}O$ records across the monsoon regions of China (X. Liu et al., 2020). In this sense, it is reasonable to assume the speleothem $\delta^{18}O$ data from Shennong Cave could represent the general trend of precipitation $\delta^{18}O$ in the region on the centennial and millennial timescales. On the whole, SZY18 δD_{C29} and Shennong stalagmite $\delta^{18}O$ exhibited similar trends over the Holocene ($r = 0.52$, $p < 0.01$), which supports a major control of δD_p on the SZY18 δD_{C29} values on the millennial timescales (Zhang, Zhang, et al., 2021; Figure 2 and Figure S4 in Supporting Information S1). Despite the overall similarity, there are apparent differences in the amplitudes. When the SZY18 δD_{C29} showed a large positive shift up to 24‰ from 4.7 to 3.8 ka (Figure 2), Shennong stalagmite $\delta^{18}O$ only oscillated within a narrow range of 1.4‰ (Zhang, Cheng, et al., 2021; Figure 2), consistent with the stalagmite $\delta^{18}O$ record from Dongge Cave (Dykoski et al., 2005) and Jiulong Cave (Zhang, Cheng, et al., 2021) in South China. Such variations are obviously smaller compared to SZY18 δD variations, given the regional meteoric water line from the nearby Fuzhou GNIP station ($\delta D = 8.52 \times \delta^{18}O + 13.30$). Together, although SZY18 δD_{C29} inherited the δD_p signal over the Holocene, it was significantly modified by other factors during 4.7 to 3.8 ka.

Changes in vegetation composition do not appear to be mainly responsible for the large shift in the SZY18 δD_{C29} record during the mid-to-late Holocene transition. Plant macrofossil data from the nearby Shuizhuyang core show a consistently overwhelming dominance (>95%) of Cyperaceae (mostly *Carex* spp.) during 4.7 to 3.8 ka, indicative of no prominent shift in vegetation assemblages (Table S2, Figure S5 and Text S1 in Supporting Information S1). Relatively high and stable percentages of Cyperaceae during this interval are also supported by the pollen record from the Shuizhuyang peat deposit (Yue et al., 2012). Consistent with the plant macrofossil and pollen results, the C_{23}/C_{29} ratio, depicting the relative proportions of different vegetation groups in peatland settings (Nichols et al., 2006; X. Huang et al., 2018), displays subtle changes during this period (Figure 2).

Accordingly, lower relative humidity with enhanced evapotranspiration (Kahmen, Hoffmann, et al., 2013; Kahmen, Schefuß, & Sachse, 2013) is the most likely factor primarily responsible for increasing δD_{C29} values from 4.7 to 3.8 ka. This assertion fits well with the amplified variations observed in the SZY18 δD_{C29} record compared to the Shennong stalagmite $\delta^{18}O$ record, as stalagmite $\delta^{18}O$ values are less or not affected by evapotranspiration. δD values of peat pore water in the upper peat layers of peatlands can be significantly enriched, as evidenced in the Dajiuhu peatland where the deeper layers were depleted up to ~20‰, indicative of apparent evaporation on the surface (Huang & Meyers, 2019). Marked evapotranspirative enrichment has also been shown for the leaf wax δD records from Dajiuhu and Hongyuan peatlands in the monsoon regions of China

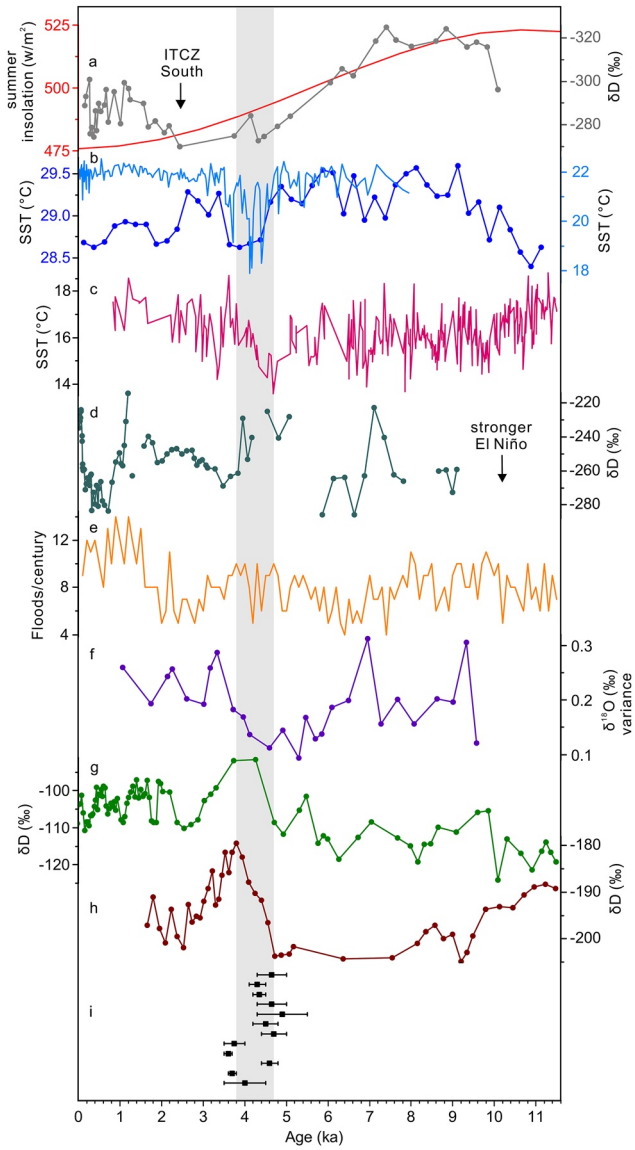

Figure 3. Comparisons of SZY18 δD_{C29} record with paleoclimate records as well as archeological data. (a) 30°N summer insolation (Berger & Loutre, 1991) (left *y*-axis) and dinosterol δD record from Palau, an indicator of the Intertropical Convergence Zone position (Sachs et al., 2018) (right *y*-axis); (b) sea surface temperature (SST) records from the western Pacific (Stott et al., 2004) (left *y*-axis) and the East China Sea (Kajita et al., 2018) (right *y*-axis); (c) SST record from the eastern Pacific (Marchitto et al., 2010); (d) Botryococcene δD record from El Junco, a proxy of El Niño activity (Zhang et al., 2014); (e) flood events per 100 years from Laguna Pallcacocha, a proxy of El Niño frequency (Mark et al., 2022); (f) foraminiferal $\delta^{18}O$ variability, IODP drill site V21-30, a proxy of ENSO variability (Koutavas & Joanides, 2012); (g) leaf wax δD record from Lake Challa (Tierney et al., 2011); (h) SZY18 δD_{C29} record; and (i) temporal distribution of mixed rice and millet farming archeological sites in Southeast China. The gray shade indicates the transitional period. Detailed information on archeological sites refers to Table S4 in Supporting Information S1.

during the Holocene (Seki et al., 2011; X. Huang et al., 2018). In addition, leaf water evaporative D-enrichment above source water was predicted to be up to 20–30‰ during the growing season on the southeast coast of China (Kahmen, Hoffmann, et al., 2013).

A drying trend from 4.7 to 3.8 ka is consistent with the hopanoid flux and pollen records from the Shuizhuyang peat deposit (X. Wang & Huang, 2019; Yue et al., 2012; Figure 2). The quite low average sedimentation rate in the SZY18 peat core during the stage before the transition might be partly due to enhanced decay under drier conditions during 4.7 to 3.8 ka (Fenner & Freeman, 2011). It is also in line with climate inference from a compilation of peat initiation records in Fujian (Lei et al., 2017). Moreover, a shift to drier conditions during the mid-to-late Holocene transition has also been suggested by paleoclimate records in Toushe Basin and Retreat Lake from Taiwan, Southeast China (Selvaraj et al., 2007; Z. Huang et al., 2020; Figure 2). The differences in the timing among the records might arise from different sensitivity of various proxies as well as differences in record resolution and dating uncertainty. Collectively, we conclude the SZY18 δD_{C29} record reveals an abrupt drying during the mid-to-late Holocene transition from 4.7 to 3.8 ka, which is a feature of the southeast coast of China.

4.2. Possible Driving Mechanisms

The abrupt drying during the mid-to-late Holocene transition on the southeast coast of China was likely modulated by the ENSO state in the tropical Pacific Ocean. During the mid-to-late Holocene transition, the Intertropical Convergence Zone migrated southward, driven by the decline of summer insolation in the North Hemisphere (Berger & Loutre, 1991; Sachs et al., 2018; Figure 3). The sea surface temperatures (SSTs) of the western Pacific Ocean and the East China Sea decreased significantly (Stott et al., 2004; Kajita et al., 2018; Figure 3). By contrast, the SSTs of the eastern Pacific Ocean displayed a remarkable increase (Marchitto et al., 2010; Figure 3). They together favored the development of a more El Niño-like state in the Pacific Ocean. Increasingly stronger El Niño has also been observed in the Botryococcene δD record from El Junco Lake (Galapagos) (Zhang et al., 2014; Figure 3). Besides, overall higher frequencies of El Niño events were recorded in Laguna Pallcacocha during the mid-to-late Holocene transition compared to the mid-Holocene (Mark et al., 2022; Figure 3). Moreover, ENSO activities have been demonstrated to become more active since ~4.5 ka after the muted state over the mid-Holocene (Du et al., 2021; Koutavas & Joanides, 2012; Figure 3). It thus appears that the hydrological shift on the southeast coast of China during the mid-to-late Holocene transition was triggered by the switch in the ENSO system with certain thresholds crossed.

Under an El Niño-like scenario, the EASM intensity would be reduced (Rao et al., 2016). The onset of the EASM would also be delayed due to the southward displacement of the westerlies (Chiang et al., 2015). The south-north displacement of the westerlies relative to the Qinghai-Tibet Plateau could modulate the hydrological changes over the EASM region by regulating the transition timing and duration of the EASM intraseasonal stages (i.e., spring, pre-Meiyu, Meiyu, and mid-summer) (Chiang et al., 2015; Zhang, Griffiths, et al., 2018). During 4.7–3.8 ka, the westerlies were positioned more southward than normal as indicated by both model simulations and paleoclimate records (Griffiths et al., 2020; Nagashima et al., 2013). The delayed northward migration of the westerlies would affect the seasonal march of the EASM rainfall, resulting in a lengthened Meiyu season in the middle and lower

reaches of the Yangtze River but a shortened mid-summer stage in North China (Chiang et al., 2015). Correspondingly, the West Pacific subtropical high (WPSH) would be enhanced and positioned more southwestward, which covered the southeast coast of China for a longer period and as such suppressed the local precipitation (Rao et al., 2016). This mechanism appears to be further supported by a brief return to more depleted δD_{C29} values after 3.8 ka, coeval with a possible shift to a more La Niña-like mean state over the tropical Pacific, as indicated by the SST records from the Pacific Ocean (Marchitto et al., 2010; Stott et al., 2004; Figure 3).

Interestingly, the drying mid-to-late Holocene transition is coincidental with the weakening of the East African monsoon revealed by the leaf wax δD record from Lake Challa (Tierney et al., 2011; Figure 3). Recent studies have highlighted the potential of the East African monsoon in modulating the ENSO mean state over the tropical Pacific Ocean, with a more El Niño-like condition under a weak East African monsoon (Griffiths et al., 2020; Pausata et al., 2017). Their covariation thus supports a dominant control of ENSO on the hydrological changes in Southeast China during the mid-to-late Holocene transition.

4.3. Potential Impact on the Regional Agriculture Development

The mid-to-late Holocene transition witnessed the southward dispersal of rice farming in South China (Yang et al., 2018). Rice, as a wetland-based crop, was the most common crop excavated from the Neolithic sites in Southeast China by far (Dai et al., 2021). Millet, as a dry crop, is considered to spread with rice. Up till now, the earliest mixed rice and millet farming in Fujian Province was found in the Baitoushan site, dating back to 5.5 ka (Dai et al., 2021). Mixed rice and millet farming has been reported to occur around 5.0 ka in the Nanguanlidong site, Southeast China (Tsang et al., 2017). These studies support that mixed rice and millet sporadically occurred in Southeast China before 5 ka or even earlier, probably as a result of the establishment of millet domestication as well as the exchange between populations from northern and southern regions. Notably, a compilation of the AMS ^{14}C dates of major sites with mixed rice and millet farming in Southeast China shows that the sites significantly increased in number and were more widely distributed after ~4.8 ka, which is generally concurrent with the abrupt drying transition documented in this study (Figure 3 and Table S4 in Supporting Information S1). In addition, the δ^{13}C data of pig remains in Pingfengshan and Huangguashan sites showed strong variations, which suggested mixed food sources from C_3 and C_4 plants as well as marine resources (Ge et al., 2019). Especially, the strong signal of C_4 plant indicative of increasing consumption of millets was dated back to 4.0–3.6 ka (Ge et al., 2019).

Compared to rice, millet is more drought-tolerant with a shorter growing season (Miller et al., 2016). In cases of severe drying, rice yield could be significantly reduced as the irrigation system probably had not been applied in the region yet (Ma et al., 2020). However, millet could cope with drier conditions. Therefore, mixed rice and millet farming might be formed in the hilly areas of the southeast coast of China to facilitate an adequate supply of food and act as an adaptation measure of human societies to climate risks. We hypothesize that the widespread mixed rice and millet farming, emerging with abrupt drying, might be triggered by the changing hydroclimate.

5. Conclusions

Hydroclimate changes on the southeast coast of China during the mid-to-late Holocene transition were reconstructed by leaf wax biomarker proxies from the Shuizhuyang peat deposit. The large positive shift in δD_{C29} reveals an abrupt drying from 4.7 to 3.8 ka, consistent with a switch in the hydrological cycle during the mid-late Holocene. This abrupt drying is likely to be shaped by a more El Niño-like mean state in the tropical Pacific Ocean, which would decrease the rainfall on the southeast coast of China due to the more southwestward position of the WPSH and its longer cover. The increasing aridity might have promoted the development of mixed rice and millet agriculture on the southeast coast of China during this critical transition.

Data Availability Statement

The data in this study are provided in Supporting Information and have been deposited in Zenodo (https://doi.org/10.5281/zenodo.7063279).

Acknowledgments
This work was supported by the National Natural Science Foundation of China (U20A2094), the Strategic Priority Research Program of Chinese Academy of Sciences (XDB26000000), the Yunnan Provincial Science and Technology Department (2019FD131), and the China Scholarship Council. Prof. Xinxin Zuo from the Fujian Normal University is thanked for his valuable comments on the late neolithic agriculture development in southeastern China. Dr. Oliver Rach is thanked for his help during sample measurements. Bingyan Zhao is thanked for his comments on the early version of this manuscript. Dr. Yu Zhou, Dr. Xudong Gou, and Sui Wan are thanked for their help in the fieldwork. Dr. Haiwei Zhang is thanked for providing stalagmite $\delta^{18}O$ data from Shennong Cave. The authors thank the anonymous reviewers for their comments that greatly improved the quality of this manuscript.

References

Andersson, R. A., Kuhry, P., Meyers, P., Zebühr, Y., Crill, P., & Mörth, M. (2011). Impacts of paleohydrological changes on *n*-alkane biomarker compositions of a Holocene peat sequence in the eastern European Russian Arctic. *Organic Geochemistry*, *42*(9), 1065–1075. https://doi.org/10.1016/j.orggeochem.2011.06.020

Berger, A., & Loutre, M. F. (1991). Insolation values for the climate of the last 10 million years. *Quaternary Science Reviews*, *10*(4), 297–317. https://doi.org/10.1016/0277-3791(91)90033-Q

Bini, M., Zanchetta, G., Perşoiu, A., Cartier, R., Català, A., Cacho, I., et al. (2019). The 4.2 ka BP event in the Mediterranean region: An overview. *Climate of the Past*, *15*(2), 555–577. https://doi.org/10.5194/cp-15-555-2019

Blaauw, M. C., & Christen, J. A. (2011). Flexible paleoclimate age-depth models using an autoregressive gamma process. *Bayesian Analysis*, *6*(3), 457–474. https://doi.org/10.1214/ba/1339616472

Chen, F., Xu, Q., Chen, J., Birks, H. J. B., Liu, J., Zhang, S., et al. (2015). East Asian summer monsoon precipitation variability since the last deglaciation. *Scientific Reports*, *5*(1), 11186. https://doi.org/10.1038/srep11186

Chen, H. F., Wen, S. Y., Song, S. R., Yang, T. N., Lee, T. Q., Lin, S. F., et al. (2012). Strengthening of paleo-typhoon and autumn rainfall in Taiwan corresponding to the Southern Oscillation at late Holocene. *Journal of Quaternary Science*, *27*(9), 964–972. https://doi.org/10.1002/jqs.2590

Chiang, J. C. H., Fung, I. Y., Wu, C.-H., Cai, Y., Edman, J. P., Liu, Y., et al. (2015). Role of seasonal transitions and westerly jets in East Asian paleoclimate. *Quaternary Science Reviews*, *108*, 111–129. https://doi.org/10.1016/j.quascirev.2014.11.009

Cullen, H. M., Demenocal, P. B., Hemming, S., Hemming, G., Brown, F. H., Guilderson, T., & Sirocko, F. (2000). Climate change and the collapse of the Akkadian empire: Evidence from the deep sea. *Geology*, *28*(4), 379–382. https://doi.org/10.1130/0091-7613(2000)28<379:CCATCO>2.0.CO;2

Dai, J., Cai, X., Jin, J., Ge, W., Huang, Y., Wu, W., et al. (2021). Earliest arrival of millet in the South China coast dating back to 5,500 years ago. *Journal of Archaeological Science*, *129*, 105356. https://doi.org/10.1016/j.jas.2021.105356

Ding, Y., & Chan, J. C. L. (2005). The East Asian summer monsoon: An overview. *Meteorology and Atmospheric Physics*, *89*(1–4), 117–142. https://doi.org/10.1007/s00703-005-0125-z

Dixit, Y., Hodell, D. A., & Petrie, C. A. (2014). Abrupt weakening of the summer monsoon in northwest India ~4100 yr ago. *Geology*, *42*(4), 339–342. https://doi.org/10.1130/G35236.1

Du, X., Hendy, I., Hinnov, L., Brown, E., Zhu, J., & Poulsen, C. J. (2021). High-resolution interannual precipitation reconstruction of Southern California: Implications for Holocene ENSO evolution. *Earth and Planetary Science Letters*, *554*, 116670. https://doi.org/10.1016/j.epsl.2020.116670

Dykoski, C. A., Edwards, R. L., Cheng, H., Yuan, D., Cai, Y., Zhang, M., et al. (2005). A high-resolution, absolute-dated Holocene and deglacial Asian monsoon record from Dongge Cave, China. *Earth and Planetary Science Letters*, *233*(1–2), 71–86. https://doi.org/10.1016/j.epsl.2005.01.036

Feakins, S. J., Bentley, L. P., Salinas, N., Shenkin, A., Blonder, B., Goldsmith, G. R., et al. (2016). Plant leaf wax biomarkers capture gradients in hydrogen isotopes of precipitation from the Andes and Amazon. *Geochimica et Cosmochimica Acta*, *182*, 155–172. https://doi.org/10.1016/j.gca.2016.03.018

Fenner, N., & Freeman, C. (2011). Drought-induced carbon loss in peatlands. *Nature Geoscience*, *4*(12), 895–900. https://doi.org/10.1038/NGEO1323

Ge, W., Yang, S., Chen, Y., Dong, S., Jiao, T., Wang, M., et al. (2019). Investigating the late neolithic millet agriculture in Southeast China: New multidisciplinary evidences. *Quaternary International*, *529*, 18–24. https://doi.org/10.1016/j.quaint.2019.01.007

Griffiths, M. L., Johnson, K. R., Pausata, F. S. R., White, J. C., Henderson, G. M., Wood, C. T., et al. (2020). End of Green Sahara amplified mid- to late Holocene megadroughts in mainland Southeast Asia. *Nature Communications*, *11*(1), 4204. https://doi.org/10.1038/s41467-020-17927-6

Huang, X., & Meyers, P. A. (2019). Assessing paleohydrologic controls on the hydrogen isotope compositions of leaf wax *n*-alkanes in Chinese peat deposits. *Palaeogeography, Palaeoclimatology, Palaeoecology*, *516*(15), 354–363. https://doi.org/10.1016/j.palaeo.2018.12.017

Huang, X., Meyers, P. A., Xue, J., Zhang, Y., & Wang, X. (2016). Paleoclimate significance of *n*-alkane molecular distributions and δ^2H values in surface peats across the monsoon region of China. *Palaeogeography, Palaeoclimatology, Palaeoecology*, *461*, 77–86. https://doi.org/10.1016/j.palaeo.2016.08.011

Huang, X., Pancost, R. D., Xue, J., Gu, Y., Evershed, R. P., & Xie, S. (2018). Response of carbon cycle to drier conditions in the mid-Holocene in central China. *Nature Communications*, *9*(1), 1369. https://doi.org/10.1038/s41467-018-03804-w

Huang, Z., Ma, C., Chyi, S. J., Tang, L., & Zhao, L. (2020). Paleofire, vegetation, and climate reconstructions of the middle to late Holocene from lacustrine sediments of the Toushe Basin, Taiwan. *Geophysical Research Letters*, *47*(20), e2020GL090401. https://doi.org/10.1029/2020gl090401

Innes, J. B., Zong, Y., Wang, Z., & Chen, Z. (2014). Climatic and palaeoecological changes during the mid- to Late Holocene transition in eastern China: High-resolution pollen and non-pollen palynomorph analysis at Pingwang, Yangtze coastal lowlands. *Quaternary Science Reviews*, *99*, 164–175. https://doi.org/10.1016/j.quascirev.2014.06.013

Kahmen, A., Hoffmann, B., Schefuß, E., Arndt, S. K., Cernusak, L. A., West, J. B., & Sachse, D. (2013). Leaf water deuterium enrichment shapes leaf wax *n*-alkane δD values of angiosperm plants II: Observational evidence and global implications. *Geochimica et Cosmochimica Acta*, *111*, 50–63. https://doi.org/10.1016/j.gca.2012.09.004

Kahmen, A., Schefuß, E., & Sachse, D. (2013). Leaf water deuterium enrichment shapes leaf wax *n*-alkane δD values of angiosperm plants I: Experimental evidence and mechanistic insights. *Geochimica et Cosmochimica Acta*, *111*, 39–49. https://doi.org/10.1016/j.gca.2012.09.003

Kajita, H., Kawahata, H., Wang, K., Zheng, H., Yang, S., Ohkouchi, N., et al. (2018). Extraordinary cold episodes during the mid-Holocene in the Yangtze delta: Interruption of the earliest rice cultivating civilization. *Quaternary Science Reviews*, *201*, 418–428. https://doi.org/10.1016/j.quascirev.2018.10.035

Koutavas, A., & Joanides, S. (2012). El Niño–Southern Oscillation extrema in the Holocene and last glacial maximum. *Paleoceanography*, *27*(4), PA4208. https://doi.org/10.1029/2012PA002378

Lei, G., Zhu, Y., Cai, B., Li, Z., Jiang, X., & Wu, J. (2017). Mid-late Holocene climate variations in Southeast China inferred by the intermountain peat records from Fujian, China. *Quaternary International*, *447*, 118–127. https://doi.org/10.1016/j.quaint.2016.09.051

Liu, F., & Feng, Z. (2012). A dramatic climatic transition at ~4000 cal. yr BP and its cultural responses in Chinese cultural domains. *The Holocene*, *22*(10), 1181–1197. https://doi.org/10.1177/0959683612441839

Liu, J., & An, Z. (2018). A hierarchical framework for disentangling different controls on leaf wax δD *n*-alkane values in terrestrial higher plants. *Quaternary Science Reviews*, *201*, 409–417. https://doi.org/10.1016/j.quascirev.2018.10.026

Liu, X., Liu, J., Chen, S., Chen, J., Zhang, X., Yan, J., & Chen, F. (2020). New insights on Chinese cave $\delta^{18}O$ records and their paleoclimatic significance. *Earth-Science Reviews*, *207*, 103216. https://doi.org/10.1016/j.earscirev.2020.103216

Ma, T., Rolett, B. V., Zheng, Z., & Zong, Y. (2020). Holocene coastal evolution preceded the expansion of paddy field rice farming. *Proceedings of the National Academy of Sciences of the United States of America*, *117*(39), 24138–24143. https://doi.org/10.1073/pnas.1919217117

Marchitto, T. M., Muscheler, R., Ortiz, J. D., Carriquiry, J. D., & Geen, A. V. (2010). Dynamical response of the tropical Pacific Ocean to solar forcing during the early Holocene. *Science*, *330*(6009), 1378–1381. https://doi.org/10.1126/science.1194887

Mark, S. Z., Abbott, M. B., Rodbell, D. T., & Moy, C. M. (2022). XRF analysis of Laguna Pallcacocha sediments yields new insights into Holocene El Niño development. *Earth and Planetary Science Letters*, *593*, 117657. https://doi.org/10.1016/j.epsl.2022.117657

McFarlin, J. M., Axford, Y., Masterson, A. L., & Osburn, M. R. (2019). Calibration of modern sedimentary δ^2H plant wax-water relationships in Greenland lakes. *Quaternary Science Reviews*, *225*, 105978. https://doi.org/10.1016/j.quascirev.2019.105978

Miller, N. F., Spengler, R. N., & Frachetti, M. (2016). Millet cultivation across Eurasia: Origins, spread, and the influence of seasonal climate. *The Holocene*, *26*(10), 1566–1575. https://doi.org/10.1177/0959683616641742

Nagashima, K., Tada, R., & Toyoda, S. (2013). Westerly jet-East Asian summer monsoon connection during the Holocene. *Geochemistry, Geophysics, Geosystems*, *14*(12), 5041–5053. https://doi.org/10.1002/2013GC004931

Nichols, J. E., Booth, R. K., Jackson, S. T., Pendall, E. G., & Huang, Y. (2006). Paleohydrologic reconstruction based on *n*-alkane distributions in ombrotrophic peat. *Organic Geochemistry*, *37*(11), 1505–1513. https://doi.org/10.1016/j.orggeochem.2006.06.020

Pausata, F. S. R., Zhang, Q., Muschitiello, F., Lu, Z., Chafik, L., Niedermeyer, E. M., et al. (2017). Greening of the Sahara suppressed ENSO activity during the mid-Holocene. *Nature Communications*, *8*(1), 16020. https://doi.org/10.1038/ncomms16020

Rach, O., Hadeen, X., & Sachse, D. (2020). An automated solid phase extraction procedure for lipid biomarker purification and stable isotope analysis. *Organic Geochemistry*, *142*, 103995. https://doi.org/10.1016/j.orggeochem.2020.103995

Rao, Z., Li, Y., Zhang, J., Jia, G., & Chen, F. (2016). Investigating the long-term palaeoclimatic controls on the δD and $\delta^{18}O$ of precipitation during the Holocene in the Indian and East Asian monsoonal regions. *Earth-Science Reviews*, *159*, 292–305. https://doi.org/10.1016/j.earscirev.2016.06.007

Reimer, P. J., Bard, E., Bayliss, A., Beck, J. W., Blackwell, P. G., Ramsey, C. B., et al. (2020). The IntCal20 northern hemisphere radiocarbon age calibration curve (0–55 cal kBP). *Radiocarbon*, *62*(4), 725–757. https://doi.org/10.1017/RDC.2020.41

Renssen, H. (2022). Climate model experiments on the 4.2 ka event: The impact of tropical sea-surface temperature anomalies and desertification. *The Holocene*, *32*(5), 378–389. https://doi.org/10.1177/09596836221074031

Sachs, J. P., Blois, J. L., McGee, T., Wolhowe, M., Haberle, S., Clark, G., & Atahan, P. (2018). Southward Shift of the Pacific ITCZ during the Holocene. *Paleoceanography and Paleoclimatology*, *33*(12), 1383–1395. https://doi.org/10.1029/2018pa003469

Sachse, D., Billault, I., Bowen, G. J., Chikaraishi, Y., Dawson, T. E., Feakins, S. J., et al. (2012). Molecular paleohydrology: Interpreting the hydrogen-isotopic composition of lipid biomarkers from photosynthesizing organisms. *Annual Review of Earth and Planetary Sciences*, *40*(1), 221–249. https://doi.org/10.1146/annurev-earth-042711-105535

Seki, O., Meyers, P. A., Yamamoto, S., Kawamura, K., Nakatsuka, T., Zhou, W., & Zheng, Y. (2011). Plant-wax hydrogen isotopic evidence for postglacial variations in delivery of precipitation in the monsoon domain of China. *Geology*, *39*(9), 875–878. https://doi.org/10.1130/G32117.1

Selvaraj, K., Chen, C. T. A., & Lou, J. Y. (2007). Holocene East Asian monsoon variability: Links to solar and tropical Pacific forcing. *Geophysical Research Letters*, *34*(1), L01703. https://doi.org/10.1029/2006GL028155

Stott, L., Cannariato, K., Thunell, R., Haug, G. H., Koutavas, A., & Lund, S. (2004). Decline of surface temperature and salinity in the western tropical Pacific Ocean in the Holocene epoch. *Nature*, *431*(7004), 56–59. https://doi.org/10.1038/nature02903

Sun, Q., Liu, Y., Wünnemann, B., Peng, Y., Chen, Z., Deng, L., et al. (2019). Climate as a factor for Neolithic cultural collapses approximately 4000 years BP in China. *Earth-Science Reviews*, *197*, 102915. https://doi.org/10.1016/j.earscirev.2019.102915

Tan, M. (2014). Circulation effect: Response of precipitation $\delta^{18}O$ to the ENSO cycle in monsoon regions of China. *Climate Dynamics*, *42*(3–4), 1067–1077. https://doi.org/10.1007/s00382-013-1732-x

Tierney, J. E., Russell, J. M., Sinninghe Damsté, J. S., Huang, Y., & Verschuren, D. (2011). Late Quaternary behavior of the East African monsoon and the importance of the Congo Air Boundary. *Quaternary Science Reviews*, *30*(7–8), 798–807. https://doi.org/10.1016/j.quascirev.2011.01.017

Tsang, C.-H., Li, K.-T., Hsu, T.-F., Tsai, Y.-C., Fang, P.-H., & Hsing, Y.-I. (2017). Broomcorn and foxtail millet were cultivated in Taiwan about 5000 years ago. *Botanical Studies*, *58*(1), 3. https://doi.org/10.1186/s40529-016-0158-2

Walker, M., Head, M. J., Berkelhammer, M., Björck, S., Cheng, H., Cwynar, L., et al. (2018). Formal ratification of the subdivision of the Holocene Series/Epoch (Quaternary System/Period): Two new Global Boundary Stratotype Sections and Points (GSSPs) and three new stages/subseries. *Episodes*, *41*(4), 213–223. https://doi.org/10.18814/epiiugs/2018/018016

Wang, M., Zheng, Z., Man, M., Hu, J., & Gao, Q. (2017). Branched GDGT-based paleotemperature reconstruction of the last 30,000 years in humid monsoon region of Southeast China. *Chemical Geology*, *463*, 94–102. https://doi.org/10.1016/j.chemgeo.2017.05.014

Wang, X., & Huang, X. (2019). Paleohydrological changes in southeastern China from 13.1 to 2.5 ka based on a multi-proxy peat record. *Palaeogeography, Palaeoclimatology, Palaeoecology*, *534*, 109282. https://doi.org/10.1016/j.palaeo.2019.109282

Weiss, H. (2016). Global megadrought, societal collapse and resilience at 4.2–3.9 ka BP across the Mediterranean and west Asia. *Past Global Change Magazine*, *24*(2), 62–63. https://doi.org/10.22498/pages.24.2.62

Xie, S., Evershed, R. P., Huang, X., Zhu, Z., Pancost, R. D., Meyers, P. A., et al. (2013). Concordant monsoon-driven postglacial hydrological changes in peat and stalagmite records and their impacts on prehistoric cultures in central China. *Geology*, *41*(8), 827–830. https://doi.org/10.1130/G34318.1

Xu, T., Sun, X., Hong, H., Wang, X., Cui, M., Lei, G., et al. (2019). Stable isotope ratios of typhoon rains in Fuzhou, Southeast China, during 2013–2017. *Journal of Hydrology*, *570*, 445–453. https://doi.org/10.1016/j.jhydrol.2019.01.017

Yang, X., Chen, Q., Ma, Y., Li, Z., Hung, H.-C., Zhang, Q., et al. (2018). New radiocarbon and archaeobotanical evidence reveal the timing and route of southward dispersal of rice farming in south China. *Science Bulletin*, *63*(22), 1495–1501. https://doi.org/10.1016/j.scib.2018.10.011

Yue, Y., Zheng, Z., Huang, K., Chevalier, M., Chase, B. M., Carré, M., et al. (2012). A continuous record of vegetation and climate change over the past 50,000 years in the Fujian Province of eastern subtropical China. *Palaeogeography, Palaeoclimatology, Palaeoecology*, *365–366*(9), 115–123. https://doi.org/10.1016/j.palaeo.2012.09.018

Zhang, H. B., Griffiths, M. L., Chiang, J. C. H., Kong, W., Wu, S., Atwood, A., et al. (2018). East Asian hydroclimate modulated by the position of the westerlies during Termination I. *Science*, *362*(6414), 580–583. https://doi.org/10.1126/science.aat9393

Zhang, H. W., Cheng, H., Cai, Y., Spötl, C., Kathayat, G., Sinha, A., et al. (2018). Hydroclimatic variations in southeastern China during the 4.2 ka event reflected by stalagmite records. *Climate of the Past*, *14*(11), 1805–1817. https://doi.org/10.5194/cp-14-1805-2018

Zhang, H. W., Cheng, H., Sinha, A., Spötl, C., Cai, Y., Liu, B., et al. (2021). Collapse of the Liangzhu and other Neolithic cultures in the lower Yangtze region in response to climate change. *Science Advances*, *7*(48), eabi9275. https://doi.org/10.1126/sciadv.abi9275

Zhang, H. W., Zhang, X., Cai, Y., Sinha, A., Spötl, C., Baker, J., et al. (2021). A data-model comparison pinpoints Holocene spatiotemporal pattern of East Asian summer monsoon. *Quaternary Science Reviews*, *261*, 106911. https://doi.org/10.1016/j.quascirev.2021.106911

Zhang, X., Jiang, X., Xiao, H., Cai, B., Yu, T.-L., & Shen, C.-C. (2021). A gradual transition into Greenland interstadial 14 in southeastern China based on a sub-decadally-resolved stalagmite record. *Quaternary Science Reviews*, *253*, 106769. https://doi.org/10.1016/j.quascirev.2020.106769

Zhang, Z., Leduc, G., & Sachs, J. P. (2014). El Niño evolution during the Holocene revealed by a biomarker rain gauge in the Galápagos Islands. *Earth and Planetary Science Letters*, *404*, 420–434. https://doi.org/10.1016/j.epsl.2014.07.013

Zhao, B., Zhang, Y., Huang, X., Qiu, R., Zhang, Z., & Meyers, P. A. (2018). Comparison of *n*-alkane molecular, carbon and hydrogen isotope compositions of different types of plants in the Dajiuhu peatland, central China. *Organic Geochemistry*, *124*, 1–11. https://doi.org/10.1016/j.orggeochem.2018.07.008

References From the Supporting Information

Barber, K. E., Chambers, F. M., Maddy, D., Stoneman, R., & Brew, J. S. (1994). A sensitive high-resolution record of late Holocene climatic change from a raised bog in northern England. *The Holocene*, *4*(2), 198–205. https://doi.org/10.1177/095968369400400209

Deng, Z., Hung, H.-C., Fan, X., Huang, Y., & Lu, H. (2018). The ancient dispersal of millets in southern China: New archaeological evidence. *The Holocene*, *28*(1), 34–43. https://doi.org/10.1177/0959683617714603

Deng, Z., Kuo, S.-C., Carson, M., & Hung, H.-C. (2022). Early Austronesians cultivated rice and millet together: Tracing Taiwan's first Neolithic crops. *Frontiers of Plant Science*, *13*, 962073. https://doi.org/10.3389/fpls.2022.962073

Deng, Z., Yan, Z., & Yu, Z. (2020). Bridging the gap on the southward dispersal route of agriculture in China: New evidences from the Guodishan site, Jiangxi province. *Archaeological and Anthropological Sciences*, *12*(7), 151–160. https://doi.org/10.1007/s12520-020-01117-y

Wan, Z., Yang, X., Ge, Q., Fan, C., Zhou, G., & Ma, Z. (2012). Plant resource utilization at Sheshantou Site in Jiangxi Province based on starch grain analysis. *Progress in Geography*, *31*, 639–645. (in Chinese with English abstract). https://doi.org/10.11820/dlkxjz.2012.05.013